Academic Journal of Electrical and Computer Engineering
Vol. 03, August 2026
https://doi.org/10.31272/ajece.40
https://ajece.uomustansiriyah.edu.iq
ISSN 3079-2878
Research Article

# Improvement of Digital Image Watermarking Algorithm Against Noise Attacks Using Dual-Tree Complex Wavelet Transform

Yasin Yousif Al-Aboosi[1*], Hussein A. Abdualnabi[2], Radhi Sehen Issa[3], Mohammed Ahmed Moh.[4]

[1,2,3] Electrical Engineering Department, College of Engineering, Mustansiriyah University, Baghdad, Iraq
[4]Scientific Research Commission / Ministry of Higher Education.
[*]Email: yasinalaboosi@uomustansiriyah.edu.iq

Received: 20/12/2025 Revised: 07/02/2026 Accepted: 21/02/2026

***Abstract*— Protecting digital images during transmission has become a fundamental requirement in modern communication systems, especially with the widespread exchange of multimedia data. Digital image watermarking is considered one of the most widely used techniques to ensure data security and protect ownership]. In this study, a robust framework for watermarking was developed by integrating the Discrete Wavelet Transform (DWT) with Singular Value Decomposition (SVD). In this paper performs transform-domain digital image watermarking, where ownership information is embedded within a host image. Although the DWT–SVD structure provides acceptable resistance to many signal processing attacks, its performance degrades significantly in the presence of additive white Gaussian noise (AWGN). To address this shortcoming, the proposed framework incorporates an additional denoising stage based on the dual-tree complex wavelet transform (DT-CWT). Due to its quasi shift-invariant characteristics and superior directional sensitivity, the DT-CWT demonstrates more effective noise reduction capabilities than traditional wavelet-based methods. Experimental evaluations indicate that the proposed method maintains high reconstruction fidelity in noisy environments, achieving a mean- squared -error (MSE) of approximately 0. 0041 and a peak- signal-to-noise ratio (PSNR) of about 70. dB. These results validate the robustness and efficiency of the proposed approach.**

**keywords—** Digital watermarking, Image denoising, DWT, SVD, Dual-tree complex wavelet transform

## I. INTRODUCTION

Digital image processing refers to the application of signal-processing-based mathematical techniques to visual information such as images and video frames, where the output may be a modified image or extracted feature information [1]. In many image processing systems, images are modeled as two-dimensional signals, allowing classical signal processing techniques to be applied effectively. Image encryption and watermarking approaches are commonly categorized into transform-domain and spatial-domain methods [2]. Pixel values are directly manipulated via spatial-domain techniques. or positions, whereas transform-domain methods embed information within frequency coefficients. Although spatial-domain approaches are straightforward, transform-domain techniques are generally favored due to their higher robustness and better imperceptibility characteristics [3], [4]. Various transform-domain watermarking methods have been reported, including DWT, DCT, FFT, and DFT [3], [4], [9]. In these approaches, watermark information is embedded by modifying selected transform coefficients. Spread-spectrum watermarking is another widely used technique, in which watermark energy is distributed over multiple frequency bands to maintain imperceptibility [1]. In this work, a hybrid watermarking and encryption scheme based on DWT and SVD is proposed [5], [6]. Although this framework demonstrates strong resistance to common attacks, its robustness decreases when the encrypted image is affected by Gaussian noise [7]. To address this issue, a DT-CWT-based denoising stage is incorporated, following recent advances in wavelet-based denoising techniques [9]–[13].

## II. DISCRETE WAVELET TRANSFORM (DWT)

Wavelet transforms are extensively used in image processing applications such as compression, watermarking, feature extraction, and denoising [2], [3]. The discrete wavelet transform provides a multi-resolution representation by decomposing an image into sub-bands corresponding to different frequency components.

### *A. Image Representation Using DWT*

An image can be represented as a two-dimensional matrix in which each element corresponds to pixel intensity [1]. Natural images typically consist of slowly varying regions along with abrupt changes that represent edges. These characteristics correspond to low-frequency and high-frequency components, respectively. The DWT effectively separates these components, allowing efficient processing and



Work of This Research is Licensed under CC BY

analysis [3]. Figure 1 illustrates multiple levels of DWT decomposition.

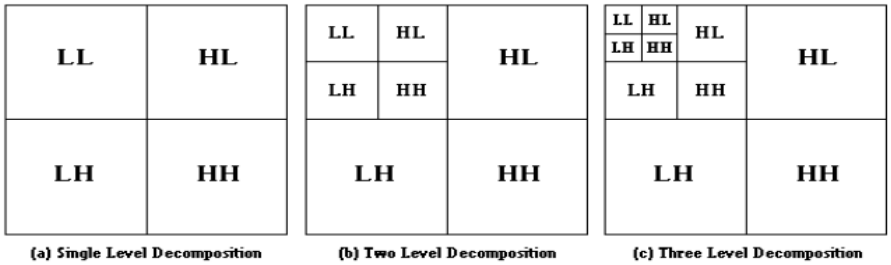



**Fig. 1.** Levels of DWT De-composition

*B. Inverse Discrete Wavelet Transform*

IDWT recover the original image by applying synthesis filters to the isolated sub-bands. This recovering process starts from the highest decomposition level and gradually restores the image resolution by the process filtering along both 2 dimensions rows and columns [2].

## III. SINGULAR VALUE DECOMPOSITION (SVD)

One method for matrix factorization is Singular Value Decomposition (SVD). that represents an image matrix as the product of three matrices.as a product of three matrices containing singular values and singular vectors [5], [6]. Unlike frequency-based transforms, SVD operates in the spatial domain; however, its singular values exhibit high stability under common image manipulations such as rotation and translation. This property makes SVD particularly suitable for watermarking and encryption applications [5], [6].

$$X = \begin{bmatrix} x_1 & x_2 \dots\dots\dots\dots & x_M \\ x_{M+1} & x_{M+2} \dots\dots\dots\dots & x_{2M} \\ x_{(K-1)M+1} & x_{(K-1)M+2\dots\dots} & x_{KM} \end{bmatrix} \quad (1)$$

SVD theorem states that MxM matrix X can be de-composed into products of the following matrices:

$$XX = U\sum V\hat{}(*\hat{}T) \quad (2)$$

Where:

$X \in \mathbb{R}^{M\times N}$ is the image matrix

$U \in \mathbb{R}^{M\times M}$ is a orethonormal matrix of LSV.

$\Sigma \in \mathbb{R}^{M\times N}$ is dieagonal matrix of SV.

$V \in \mathbb{R}^{N\times N}$ is a orethonormal matrix of RSV.

Singular values exhibit high stability under common image processing operations, making SVD suitable for watermark embedding.

$$U = \begin{bmatrix} 1 & 1 \dots\dots & 1 \\ u_1 & u_2 \dots\dots & u_K \\ 1 & 1 \dots\dots & 1 \end{bmatrix} \quad (3)$$

V represent MxM orethonormal matrix associated with RSV,

$$V = \begin{bmatrix} 1 & 1 \dots\dots & 1 \\ v_1 & v_2 \dots\dots & v_K \\ 1 & 1 \dots\dots & 1 \end{bmatrix} \quad (4)$$

whereas $\sum$ represent KxM matrix with regard to non-negative RSV:

$$\Sigma = \begin{bmatrix} \sigma_1 & 0 & \dots & 0 \\ 0 & \sigma_2 & \dots & 0 \\ \cdot & \cdot & \cdot & \cdot \\ \cdot & \cdot & \cdot & \cdot \\ \cdot & \cdot & \cdot & \cdot \\ 0 & 0 & \dots & \sigma_M \\ 0 & 0 & \dots & 0 \\ \cdot & \cdot & \cdot & \cdot \\ \cdot & \cdot & \cdot & \cdot \\ \cdot & \cdot & \cdot & \cdot \\ 0 & 0 & \dots & 0 \end{bmatrix}. \quad (5)$$

Based on this stability, numerous watermarking schemes embed watermark information by slightly modifying singular values. More recent hybrid approaches combine SVD with DWT or DCT to further enhance robustness against attacks [9].

## IV. DUAL-TREE COMPLEX WAVELET TRANSFORM.

The dual-tree complex wavelet transform employs two parallel wavelet filter banks that form a Hilbert transform pair, commonly referred to as real and imaginary trees [14]. This structure enables near shift-invariant signal representation and improved directional selectivity compared with the conventional DWT. as illustrated in Figure 2.

$$\psi_{im} = \mathrm{H}\{\psi_{re}\} = \begin{cases} -j\,\psi_{re} & \omega \geq 0 \\ j\,\psi_{re} & \omega < 0 \end{cases} \quad (6)$$

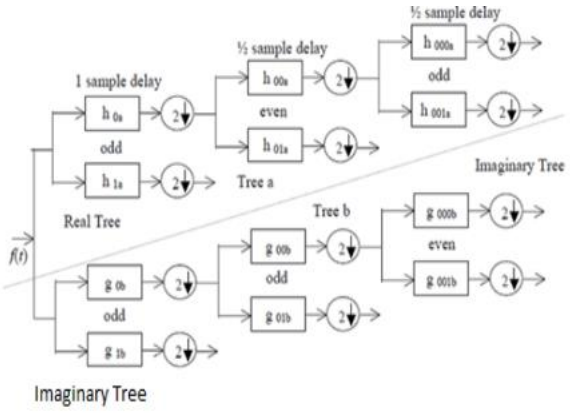



**Fig. 2.** The Complex Wavelet Transform Analysis filter.

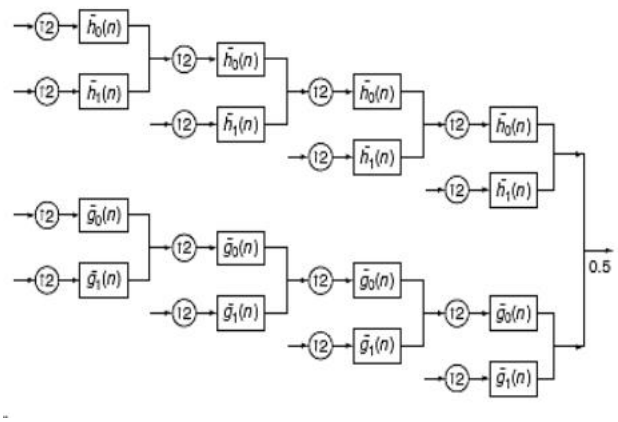



**Fig. 3.** Complex wavelet transform synthesizer filter.

Due to these properties, DT-CWT provides superior reconstruction accuracy and enhanced noise suppression capabilities, making it suitable for image denoising applications [14], [15]. Figure 3 illustrates the synthesis filter structure used for inverse DT-DWT.

$$w0(n) = e0\left(n - \frac{1}{2}\right) \quad (7)$$

Equation (11) can be expressed in Fourier transform:

$$W0(\omega) = E0(\omega)\, e^{-j\theta(\omega)} \quad (8)$$

Where $\theta(\omega) = \frac{\omega}{2}\ ,\ |\omega| < \pi$

## V. IMAGE DENOISING USING DT-CWT

Digital images are often corrupted by noise during acquisition or transmission, which degrades subsequent processes such as feature extraction and decryption [7]. Additive white Gaussian noise is among the most common noise models encountered in practice [8].

In the proposed approach, the noisy image is transformed using DT-CWT [13]. The real and imaginary components of the wavelet coefficients are then subjected to thresholding separately. To reduce noise while maintaining crucial image information, both hard and soft thresholding techniques are employed [10]–[13].The denoised image is finally reconstructed using the inverse DT-CWT, as illustrated in Figure 4

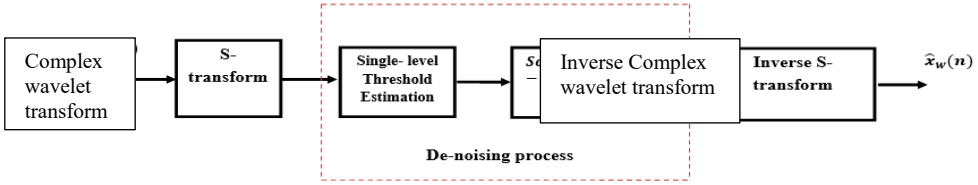



**Fig.4.** Flow graph of denoising process.

A noisy image corrupted by additive white Gaussian noise (AWGN) is first transformed using DT-DWT:

$$X(n,k) = \sum_{m=0}^{N-1} x(m - n) e^{\frac{-2\pi^2 m^2}{k^2}} e^{\frac{-j2\pi mk}{N}} = \sum_{m=0}^{N-1} x(m - n) w(m)\, e^{\frac{-j2\pi mk}{N}} = X(k) \underset{(k)}{*} W(k) e^{-j\frac{2\pi nk}{N}} \quad ((9)$$

In the case where the image is regarded in the terms of the imagenary andreal components, Equation12 may be denoted as follows:

$$X(n,k) = [X_{re}(k) + jX_{im}(k)] \underset{(k)}{*} W(k) e^{-j\frac{2\pi nk}{N}} = \left[X_{re}(k) \underset{(k)}{*} W(k) e^{-j\frac{2\pi nk}{N}} + jX_{im}(k) \underset{(k)}{*} W(k) e^{-j\frac{2\pi nk}{N}}\right] \quad ((10)$$

The complex exponential denotes by $(e^{-j\frac{2\pi nk}{N}})$ signifies temporal domain window shift. Equation (13)

indicates that the frequency domain denoising procedure necessitates thresholding in both the imaginary and real components of the spectrum. The threshold value is computed as follows:

$$\gamma_{k,re} = \xi . \sigma_{v,k,re}\sqrt{2log(N)}$$
$$\gamma_{k,im} = \xi . \sigma_{v,k,im}\sqrt{2log(N)} \quad (11)$$

In which $\sigma_{v,k,re}$and $\sigma_{v,k,im}$ are the noise standard deviations for the real and imaginary components, respectively. The values of the kth noise standard deviation can be computed based on:

$$\sigma_{v,k,re} = \frac{median(|X_{re}(n,k)|)}{0.6745}$$
$$\sigma_{v,k,im} = \frac{median(|X_{im}(n,k)|)}{0.6745} \quad (12)$$

Following threshold value for imagenary and realparts $\gamma_{k,im}$ and $\gamma_{k,re}$ the time - frequency representations of imagenary and realparts after hard thresholding include:

$$X_{\gamma,re}(n,k) = \begin{cases} X_{re}(n,k) & if|X_{re}(n,k)| > \gamma_{k,re} \\ 0 & if|X_{re}(n,k)| \le \gamma_{k,re} \end{cases}$$
$$X_{\gamma,im}(n,k) = \begin{cases} X_{im}(n,k) & if|X_{im}(n,k)| > \gamma_{k,im} \\ 0 & if|X_{im}(n,k)| \le \gamma_{k,im} \end{cases} \quad (13)$$

After soft - thresholding, time-frequency representation of imagenary and realparts can be show as:

$$X_{\gamma,re}(n,k) = \begin{cases} sgn(X_{re}(n,k))\left(|X_{re}(n,k)| - \gamma_{k,re}\right) & if|X_r \\ 0 & if|X_{re} \end{cases}$$
$$X_{\gamma,im}(n,k) = \begin{cases} sgn(X_{im}(n,k))(|X_{im}(n,k)| - \gamma_{k,im}) & if|X \\ 0 & if|X \end{cases} \quad (14)$$

Combining imaginary and real parts yields the following time-frequency representation:

$$X_{\gamma}(n,k) = X_{\gamma,re}(n,k) + jX_{\gamma,im}(n,k) \quad (15)$$

## VI. PROPOSED WATERMARKING AND ENCRYPTION FRAMEWORK

All experiments were conducted using standard grayscale images (Lena, Peppers, Cameraman) of size 512 × 512 pixels with intensity range [0, 255]. Watermark images were resized to match host dimensions. Gaussian noise with variance levels 0.01, 0.05, and 0.1 was evaluated. To improve resistance against noise attacks, denoising is performed prior to the decryption stage [7], [13]. The overall encryption–decryption workflow consists of the following steps also the proposed encryption–decryption workflow is illustrated in Figure 5.

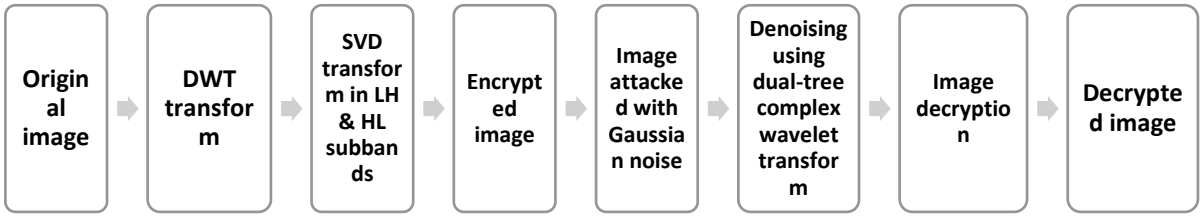



**Fig. 5.** Suggested model

The encryption–decryption process follows these steps:, according to Fig.5:

The procedure is summarized as follows:

1. Selection of host and original images with identical dimensions.
2. Application of DWT and SVD to the image sub-bands [5], [6].
3. Generation of the encrypted image using inverse DWT
4. Transmission through a noisy channel.
5. DT-CWT-based denoising.
6. Image decryption to recover the original content

## VII. PERFORMANCE MESEUREMENTS

The performance of proposed method is evaluated using MAE, NMSE, MSE, and PSNR. A PSNR value above 40 dB indicates high-quality reconstruction, whereas values below 20 dB correspond to poor image quality [14], [16].

$$PSNR = 10\ \log_{10}\frac{255^2}{MSE} \quad (16)$$

Where MSE denotes errors between the original - image ($x$) and denoised one ($\hat{x}$) with an MxN size:

$$MSE = \frac{1}{M*N}\sum_{i=1}^{M}\sum_{j=1}^{N}[x(i,j) - \hat{x}(i,j)]^2 \quad (17)$$

## VIII. RESULTS AND DISCUSSIONS

Experiments were conducted using standard grayscale images (Lena, Peppers, Cameraman) of size 512×512. Noise Gaussen

variances of 0.01, 0.05, & 0.1 were tested. DT-CWT-based denoising consistently outperformed conventional DWT denoising, achieving a PSNR of 70.015 dB at variance 0.1.

Three experimental cases are investigated: watermarking without noise, watermarking with Gaussian noise using DWT denoising, and watermarking with Gaussian noise using DT-CWT denoising [7], [13]. The results confirm that DT-CWT-based denoising significantly outperforms conventional DWT denoising in terms of PSNR and MSE. Visual inspection further shows that the encrypted images maintain strong similarity to the host image, while the decrypted images accurately recover the embedded content [5], [6].

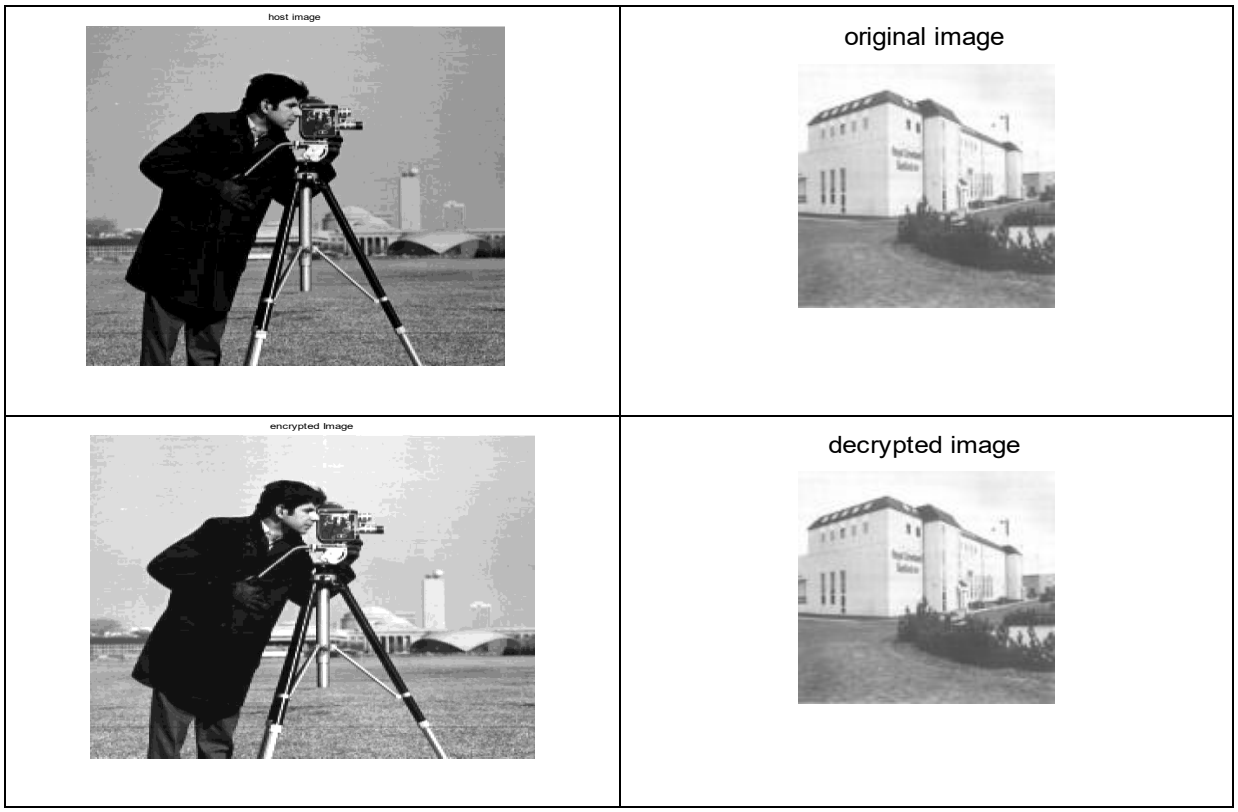
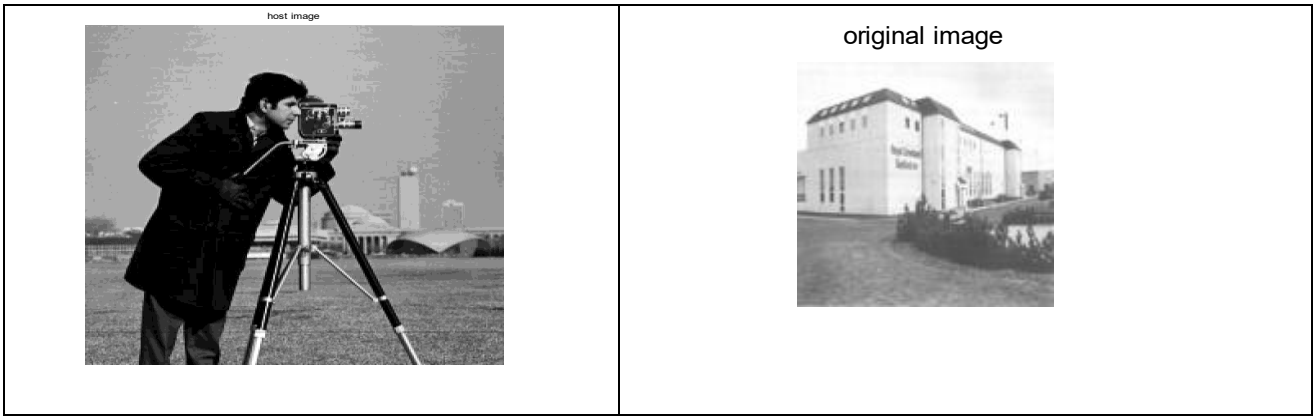



**Fig. 6**. Results for image encryption without noise attacks.

The DWT-SVD noise method was utilized to embed the original image within the host image. A Gaussian image with variance attacks was later applied to the watermark image, followed by the elimination of the attack noise via the DWT technique. Subsequently, it was dewatered, and the resultant water-marked image is depicted in Figure. 6.



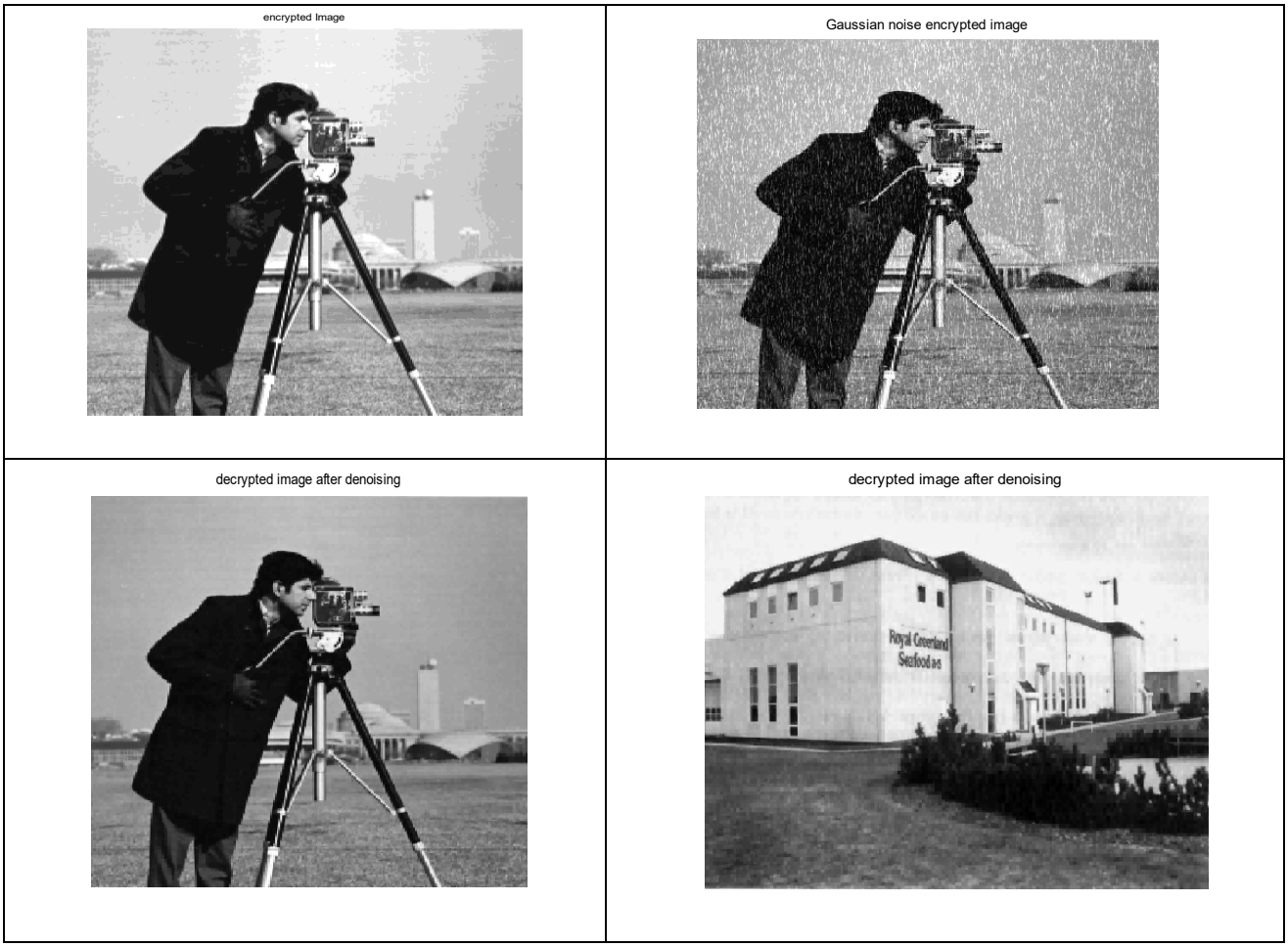



**Fig. 7**. results of gauss noise attacks were used to encrypt images, and the DWT technique was used for decryption.

Although this study focuses on Gaussian noise attacks, future work will extend evaluation to salt-and-pepper noise, JPEG compression, and filtering attacks to further validate robustness. The original image was watermarked on the host image using the DWT-SVD noise approach. The water-marked image is shown in Figure 7 after a Gaussian image with variance attack was applied to it, the attack noise was removed using the dual-tree complex wavelet transform algorithm, and it was then dewatered.



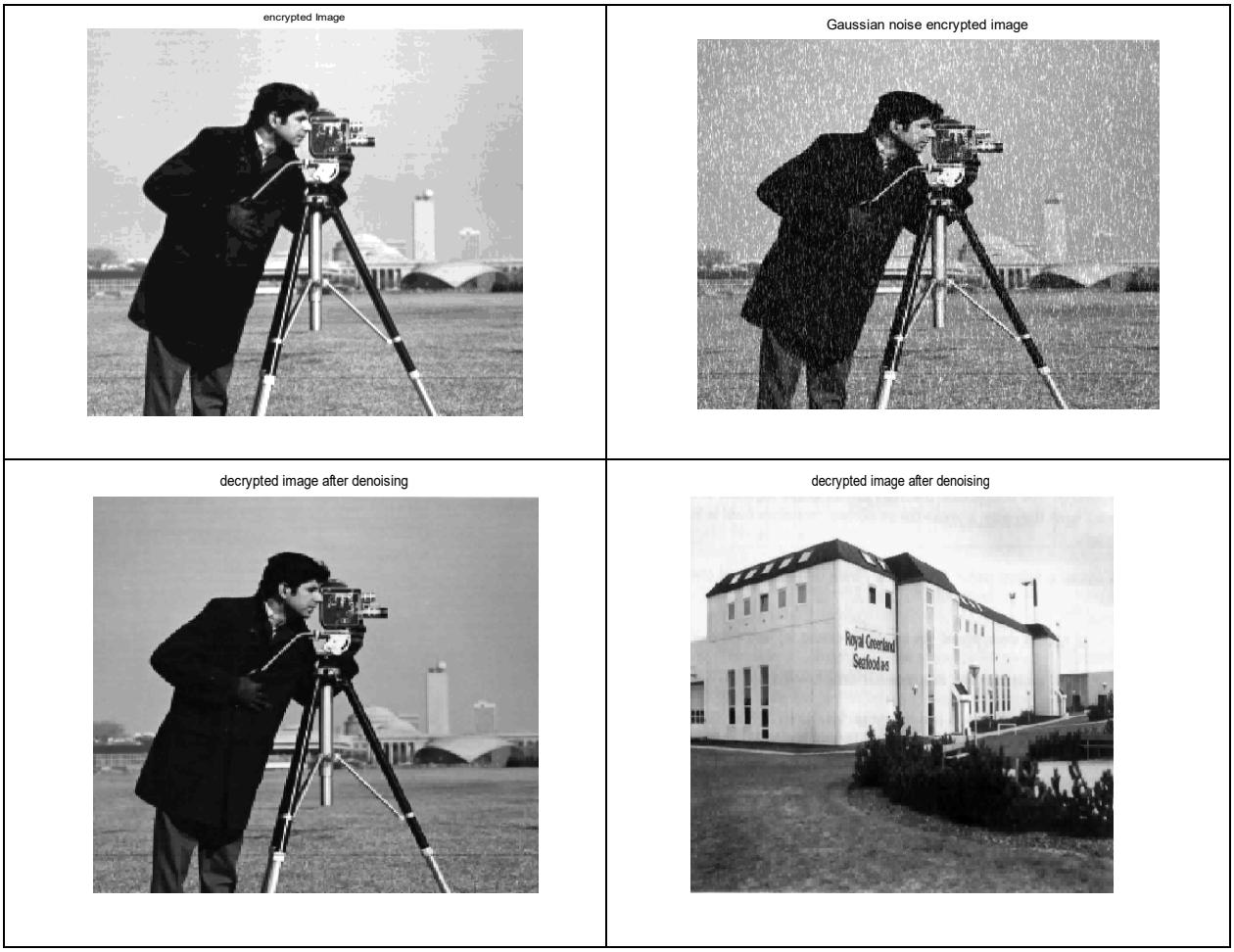



**Fig. 8.** outcomes of using the dual-tree complex wavelet transform algorithm for decryption and Gaussian noise assaults for picture encryption.

In contrast to the case without noise interference and the DWT-based denoising methodology, Table I assesses the effectiveness of the suggested method using the DT-CWT-Based Denoising algorithm on noise power with a variance of 0.1. MSE and PSNR values are calculated using the noise power value.

Table I – comparision between the proposed algorithm and another method

| Method | Noise Variance | PSNR (dB) | MSE |
|---|---|---|---|
| **No Attack** | 0 | ∞ (Not Applicable) | 0 |
| **DWT-Based Denoising** | 0.1 | 38.50 | 0.006 |
| **DT-CWT-Based Denoising** | 0.1 | 70.015 | 0.004 |

## IX. CONCLUSIONS

This work demonstrates that integrating DT-CWT-based denoising with a hybrid DWT–SVD watermarking framework significantly enhances robustness against Gaussian noise attacks. Quantitative evaluation using PSNR and MSE confirms superior reconstruction quality compared with conventional DWT-based denoising techniques, validating the effectiveness of the proposed approach for secure image transmission.

**REFERENCES:**

[1] Al-Aboosi, Y.Y., R.S. Issa, and A. khalid Jassim, Image denosing in underwater acoustic noise using discrete wavelet transform with different noise level estimation.
[2] Misiti, M., et al., Wavelet toolbox. The MathWorks Inc., Natick, MA, 1996. 15: p. 21.
[3] Gupta, D. and S. Choubey, Discrete wavelet transform for image processing. International Journal of Emerging Technology and Advanced Engineering, 2015. 4(3): p. 598-602.
[4] Baleanu, D., Advances in wavelet theory and their applications in engineering, physics and technology. 2012: BoD–Books on Demand.
[5] Makbol, N.M., B.E. Khoo, and T.H. Rassem, Block-based discrete wavelet transform-singular value decomposition image watermarking scheme using human visual system characteristics. IET Image processing, 2016. 10(1): p. 34-52.
[6] Mansouri, A., A.M. Aznaveh, and F.T. Azar, SVD-based digital image watermarking using complex wavelet transform. Sadhana, 2009. 34(3): p. 393-406.
[7] Abdulwahed, M.N. and A.K. Ahmed, Improved anti-noise attack ability of image encryption algorithm using de-noising technique. TELKOMNIKA (Telecommunication Computing Electronics and Control), 2020. 18(6): p. 3080-3087.
[8] Cloutier, M.A., Optimal Digital Detection of Acoustic Signals in Colored Noise. 1995, NAVAL POSTGRADUATE SCHOOL MONTEREY CA.
[9] Mitra, D.S. and M.A.K. Saxena, DCT DWT SVD Image Watermarking. 2018.

[10] Stockwell, R.G., L. Mansinha, and R. Lowe, Localization of the complex spectrum: the S transform. Signal Processing, IEEE Transactions on, 1996. 44(4): p. 998-1001.
[11] Pinnegar, C.R. and D.W. Eaton, Application of the S transform to prestack noise attenuation filtering. Journal of Geophysical Research: Solid Earth (1978–2012), 2003. 108(B9).
[12] Schimmel, M. and J. Gallart, The inverse S-transform in filters with time-frequency localization. Signal Processing, IEEE Transactions on, 2005. 53(11): p. 4417-4422.
[13] Abdulwahed, M.N. and A.K. Ahmed, Underwater image de-nosing using discrete wavelet transform and pre-whitening filter. TELKOMNIKA (Telecommunication Computing Electronics and Control), 2018. 16(6): p. 2622-2629.
[14] Tan, C., et al., A novel application of range-gated underwater laser imaging system (ULIS) in near-target turbid medium. Optics and Lasers in Engineering, 2005. 43(9): p. 995-1009.
[15] Ellinas, J., et al., Image de-noising using wavelets. TEI of Piraeus Applied Research Review, 2004. 9(1): p. 97-109.